


Thermodynamic instability of nonlinearly charged black holes in gravity's rainbow

S. H. Hendi^{1,2,a} , S. Panahiyan^{1,3,b}, B. Eslam Panah^{1,c}, M. Momennia^{1,d}

¹ Physics Department and Biruni Observatory, College of Sciences, Shiraz University, Shiraz 71454, Iran

² Research Institute for Astronomy and Astrophysics of Maragha (RIAAM), P.O. Box 55134-441, Maragha, Iran

³ Physics Department, Shahid Beheshti University, Tehran 19839, Iran

Received: 13 November 2015 / Accepted: 29 February 2016 / Published online: 17 March 2016
© The Author(s) 2016. This article is published with open access at Springerlink.com

Abstract Motivated by the violation of Lorentz invariance in quantum gravity, we study black hole solutions in gravity's rainbow in the context of Einstein gravity coupled with various models of nonlinear electrodynamics. We regard an energy dependent spacetime and obtain the related metric functions and electric fields. We show that there is an essential singularity at the origin which is covered by an event horizon. We also compute the conserved and thermodynamical quantities and examine the validity of the first law of thermodynamics in the presence of rainbow functions. Finally, we investigate the thermal stability conditions for these black hole solutions in the context of canonical ensemble. We show that the thermodynamical structure of the solutions depends on the choices of nonlinearity parameters, charge, and energy functions.

1 Introduction

One of the dreams of physicists is finding a consistent quantum theory of gravity. Although there are a lot of attempts to conjoin gravity and quantum theories, there is no complete description of quantum gravity. On the other hand, it has been shown that the violation of Lorentz invariance is an essential primitive rule to construct a quantum theory of gravity. The Lorentz invariance violation may be expressed in the form of modified dispersion relations [1–5]. Indeed, regarding various approaches of quantum gravity, there is evidence which shows that the Lorentz symmetry might be violated in the ultraviolet limit [6–10], and then it only holds in the infrared limit of the quantum theory of gravity. Since

the standard energy-momentum dispersion relation enjoys the Lorentz symmetry, it is expected to modify this relation in the ultraviolet limit. In fact, it has been observed that such a modification to the standard energy-momentum relation occurs in some models based on string theory [1], the spin network in loop quantum gravity (LQG) [2], spacetime foam [4], the discrete spacetime [5], Horava–Lifshitz gravity [11, 12], ghost condensation [13], non-commutative geometry [3, 14], and doubly special relativity.

In doubly special relativity, there are two fundamental constants; the velocity of light and the Planck energy. In this theory, it is not possible for a particle to attain an energy and velocity larger than the Planck energy and the velocity of light, respectively. The doubly special relativity has been generalized to curved spacetime, and this doubly general theory of relativity is called gravity's rainbow [15, 16]. In gravity's rainbow, the energy of the test particle affects the geometry of spacetime. It means that gravity has different effects on the particles with various energies. Hence, the geometry of spacetime is represented by a family of energy dependent metrics forming a rainbow of metrics. The gravity's rainbow can be constructed by considering the following deformation of the standard energy-momentum relation:

$$E^2 f^2(\varepsilon) - p^2 g^2(\varepsilon) = m^2, \quad (1)$$

where $\varepsilon = E/E_P$ and E_P is the Planck energy. The functions $f(\varepsilon)$ and $g(\varepsilon)$ are called rainbow functions and they are phenomenologically motivated. The rainbow functions are required to satisfy

$$\lim_{\varepsilon \rightarrow 0} f(\varepsilon) = 1, \quad \lim_{\varepsilon \rightarrow 0} g(\varepsilon) = 1. \quad (2)$$

where this condition ensures that we have the standard energy-momentum relation in the infrared limit. It is worthwhile to mention that the spacetime is probed at an energy E , and by definition this cannot be greater than the Planck energy E_P . It means that if a test particle is used to probe

^a e-mail: hendi@shirazu.ac.ir

^b e-mail: sh.panahiyan@gmail.com

^c e-mail: behzad.eslampanah@gmail.com

^d e-mail: momennia1988@gmail.com

the geometry of spacetime, then E is the energy of that test particle, and so E cannot become larger than E_P [17]. It is worth mentioning that such a justification is based on the standard model of particle physics. In other words, if a particle is described by the standard model, the upper limit of the Planck energy is enforced and energy functions will have to satisfy mentioned condition, whereas in trans-planckian physics such a condition could be violated. It means that the particle probing spacetime could acquire energies larger than the Planck energy. Such a property has been considered and employed in a number of papers [18–23]. This consideration requires modifications in the structure of the energy functions as well. However, we will conduct our study with consideration of the standard model and the mentioned conditions for energies that the particle could acquire. Now, it is possible to define an energy dependent deformation of the metric \hat{g} [17],

$$\hat{g} = \eta^{\mu\nu} e_\mu(E) \otimes e_\nu(E), \quad (3)$$

where

$$e_0(E) = \frac{1}{f(\varepsilon)} \hat{e}_0, \quad e_i(E) = \frac{1}{g(\varepsilon)} \hat{e}_i, \quad (4)$$

in which the hatted quantities refer to the energy independent frame.

In recent years, the effects of gravity's rainbow have been investigated in the context of black hole thermodynamics in the literature [24–27]. The modification in the thermodynamics of black rings and other black objects in the context of gravity's rainbow has been investigated in [28, 29]. In addition, the hydrostatic equilibrium equation in Einstein gravity's rainbow has been obtained and the maximum mass of neutron stars has been investigated in Ref. [30]. As we consider black holes in gravity's rainbow, the energy E corresponds to the energy of a quantum particle in the neighborhood of the event horizon, which is emitted in the Hawking radiation [24, 31–34]. On the other hand, gravity's rainbow holds the usual uncertainty principle [35, 36]. It is possible to translate the uncertainty principle $\Delta p \geq 1/\Delta x$ into a bound on the energy $E \geq 1/\Delta x$, in which E can be interpreted as the energy of a particle emitted in the Hawking radiation. It has been shown that the uncertainty in the position of a test particle in the vicinity of the horizon should be equal to the event horizon radius [24, 31–34]

$$E \geq 1/\Delta x \approx 1/r_+, \quad (5)$$

where E is the energy of a particle near the horizon, which is bounded by the Planck energy E_P and cannot increase to arbitrary values. This bound on the energy modifies temperature and entropy of the black hole in gravity's rainbow [24].

Now, we present various motivations for considering nonlinear electrodynamics. As we know, most physical systems are inherently nonlinear in nature and nonlinear field theories are appropriate tools to investigate such systems.

The main reason to consider the nonlinear electrodynamics (NED) comes from the fact that these theories are considerably richer than the Maxwell theory and in special cases they reduce to the linear Maxwell field. In addition, some limitations of the Maxwell field, such as radiation inside specific materials [37–40] and the description of the self-interaction of virtual electron–positron pairs [41–43], motivate one to regard NED [44, 45]. Also, taking into account the NED, one can remove both the big bang and the black hole singularities [46–51]. One can find regular black hole solutions of Einstein gravity in the presence of a suitable NED [46, 47, 52–55]. Moreover, the effects of NED become indeed very important in superstrongly magnetized compact objects, such as pulsars and neutron stars [56–58]. In addition, horizonless magnetic solutions in the presence of different nonlinear electromagnetic fields have been investigated in the literature [59, 60]. Besides, an interesting property which is common to all NED models is the fact that black object solutions coupled to the NED models enjoy the zeroth and first laws of thermodynamics.

It is well known that the electric field of a point-like charge has a divergency in the origin. To remove this singularity, about 80 years ago Born and Infeld introduced an interesting kind of NED which is known as Born–Infeld (BI) nonlinear electrodynamics (BINED) theory [61, 62]. Then Hoffmann tried to couple the NED with gravity [63]. The gravitational fields coupled to BINED have been investigated for static black holes [64–69], rotating black objects [70–74], wormholes [75–78], and superconductors [79–84]. Also, BINED has acquired a new impetus, since it naturally arises in the low-energy limit of the open string theory [85–90]. Recently, two different BI type models of the NED with logarithmic [52] and exponential forms [91] have been introduced, which can also remove the divergency of the electric field near the origin. The logarithmic NED (LNED), like BI theory, removes the divergency of the electric field, while the exponential NED (ENED) does not cancel the divergency, but its singularity is much weaker than that in the Maxwell theory. Black object solutions coupled to LNED and ENED have been studied in the literature (e.g., see [78, 92, 93]). Despite the BI type models, another example of NED is power Maxwell invariant (PMI) field [94–100]. The basic motivation of regarding PMI theory comes from the fact that it is interesting to modify Maxwell theory in such a way that its corresponding energy-momentum tensor will be conformally invariant. Taking into account the traceless energy-momentum tensor of electrodynamics, one should regard a conformally invariant Maxwell field which is a subclass of PMI theory.

In this paper, we will study the thermal stability of black holes in gravity's rainbow and see how the presence of rainbow functions modifies the stability conditions and phase transition of black holes. Thermodynamical aspects of black

holes have been among the most interesting subjects since the pioneering work of Hawking and Beckenstein [101–103]. The analogy between geometrical properties of the black holes and thermodynamical variables presents a deep insight into relations between the physical properties of gravity and classical thermodynamics. Due to this fundamental relation, it is believed that a consistent theory of quantum gravity could be derived through the use of the thermodynamics of black holes. One of the important subjects of black hole thermodynamics is thermal stability. In thermal stability the positivity of the heat capacity determines whether the black holes are thermally stable. In addition, the divergency of the heat capacity is where a black hole meets a second order phase transition [104, 105]. Recently, it was shown that divergencies of the heat capacity also coincide with phase transitions that are observed in extended phase space [106].

The outline of the paper is as follows. The next section is devoted to the introduction of the field equations and their related metric functions. In Sect. 3, conserved and thermodynamic quantities will be obtained and the validity of the first law of thermodynamics will be examined. Then the stability of the solutions and the phase transition are investigated through the canonical ensemble. This paper will finish with some final remarks.

2 Field equations and metric function

The metric describing gravity’s rainbow is constructed by considering the effects of energy of a particle. In other words, using doubly general relativity and parameterizing spacetime with the ratio of $\varepsilon = E/E_p$, one can construct a rainbow spacetime. Interestingly, this metric contains specific restriction with regard to mentioned ratio which will be stated later. Considering mentioned method for building up metric, one can have the rainbow metric in the following form in four dimensions:

$$d\tau^2 = -ds^2 = \frac{\Psi(r)}{f(\varepsilon)^2} dt^2 - \frac{1}{g(\varepsilon)^2} \left(\frac{dr^2}{\Psi(r)} + r^2 d\Omega_k^2 \right), \tag{6}$$

where $d\Omega_k^2$ represents the line elements of 2-dimensional hypersurfaces with the constant curvature $2k$ and the volume V_2 in the following form:

$$d\Omega_k^2 = \begin{cases} d\theta^2 + \sin^2 \theta d\varphi^2 & k = 1, \\ d\theta^2 + \sinh^2 \theta d\varphi^2 & k = -1, \\ d\theta^2 + d\varphi^2 & k = 0, \end{cases} \tag{7}$$

in which a 2-dimensional hypersurface with plane, spherical, and hyperbola symmetries are, respectively, denoted by $k = 0, k = 1$, and $k = -1$.

Our goal is to obtain rainbow solutions in Einstein gravity with cosmological constant in the presence of NED. So the total Lagrangian for this system is

$$L_{\text{total}} = L_E - 2\Lambda + L(\mathcal{F}), \tag{8}$$

in which the Lagrangian of Einstein gravity is $L_E = R$, and Λ refers to the cosmological constant. The last term in Eq. (8) is the Lagrangian of NED, which we consider to be of the following form:

$$L(\mathcal{F}) = \begin{cases} 4\beta^2 \left(1 - \sqrt{1 + \frac{\mathcal{F}}{2\beta^2}} \right), & \text{BINED,} \\ \beta^2 \left[\exp\left(-\frac{\mathcal{F}}{\beta^2}\right) - 1 \right], & \text{ENED,} \\ -8\beta^2 \ln\left(1 + \frac{\mathcal{F}}{8\beta^2}\right), & \text{LNED,} \\ (-\mathcal{F})^s, & \text{PMI,} \end{cases} \tag{9}$$

where β and s are nonlinearity parameters, the Maxwell invariant is $\mathcal{F} = F_{ab}F^{ab}$ in which $F_{ab} = \partial_a A_b - \partial_b A_a$ is the electromagnetic field tensor, and A_b is the gauge potential. It is worthwhile to mention that in essence BINED, ENED, and LNED are categorized under a same branch and they are called BI type models of NED. The series expansion of BI type models for large values of nonlinearity parameter yields similar results: the first term is Maxwell invariant which is related to Maxwell theory of electromagnetic field, the second term is quadratic Maxwell invariant coupled with nonlinearity parameter and some factors which depend on theory under consideration (for explicit forms of the expansion see Ref. [91]). On the other hand, PMI has a different structure and properties comparing to BI type models. In order to recover the Maxwell field, one should set $s = 1$.

Now, we are in a position to obtain field equations. Applying the variational principle to the Lagrangian (8), one can find

$$\nabla_a \left(\sqrt{-g} L_{\mathcal{F}} F^{ab} \right) = 0, \tag{10}$$

$$\Lambda g_{ab} + G_{ab}^{(E)} = \frac{1}{2} g_{ab} L(\mathcal{F}) - 2L_{\mathcal{F}} F_{ac} F_b^c, \tag{11}$$

where $L_{\mathcal{F}} = \frac{dL(\mathcal{F})}{d\mathcal{F}}$ and $G_{ab}^{(E)} = R_{ab} - \frac{1}{2} g_{ab} R$.

Next, due to our interest in electrically charged black holes in gravity’s rainbow, we consider a radial electric field of which the related gauge potential is

$$A_b = h(r) \delta_b^t. \tag{12}$$

Using Eqs. (6), (9), and (10), we obtain the following differential equations:

$$\begin{aligned} r\beta^2 H' - 2f(\varepsilon)^2 g(\varepsilon)^2 H^3 + 2\beta^2 H &= 0, & \text{BINED,} \\ r\beta^2 H' + 4rf(\varepsilon)^2 g(\varepsilon)^2 H^2 + 2\beta^2 H &= 0, & \text{ENED,} \\ (4r\beta^2 + rf(\varepsilon)^2 g(\varepsilon)^2 H^2) H' \\ + 8H\beta^2 - 2f(\varepsilon)^2 g(\varepsilon)^2 H^3 &= 0, & \text{LNED,} \\ 2H + (2rs - 1) H' &= 0, & \text{PMI,} \end{aligned} \tag{13}$$

in which $H = H(r) = \frac{dh(r)}{dr}$, and the prime denotes derivation with respect to the radial coordinate. It is a matter of calculation to show that

$$H(r) = \begin{cases} \frac{q}{r^2\Gamma}, & \text{BINED,} \\ \frac{q}{r^2} \exp\left(-\frac{1}{2}L_w\right), & \text{ENED,} \\ \frac{2\beta^2 r^2}{qf(\epsilon)^2 g(\epsilon)^2} (\Gamma - 1), & \text{LNED,} \\ \frac{q}{r^{2s-1}}, & \text{PMI,} \end{cases} \quad (14)$$

where $L_w = \text{LambertW}\left(\frac{4q^2 f(\epsilon)^2 g(\epsilon)^2}{\beta^2 r^4}\right)$, $\Gamma = \sqrt{1 + \frac{q^2 f(\epsilon)^2 g(\epsilon)^2}{\beta^2 r^4}}$, and q is an integration constant related to the electric charge. In order to have a well-defined solution with a PMI source, we should consider the PMI parameter, s , larger than $1/2$ ($s > 1/2$).

By employing Eqs. (6), (11), and (14), one can find the metric function for gravity's rainbow in the presence of the mentioned NED,

$$\Psi(r) = k - \frac{m}{r} - \frac{\Lambda r^2}{3g(\epsilon)^2} + \Upsilon, \quad (15)$$

$$T = \begin{cases} \frac{kr_+^2 g(\epsilon)^2 - 2r_+^4 \Lambda + 2\beta^2 r_+^4 (1 - \mathfrak{F}_{1+}) - 4q^2 f(\epsilon)^2 g(\epsilon)^2 \mathfrak{F}_{2+}}{4\pi f(\epsilon) g(\epsilon) r_+^3}, & \text{BINED,} \\ \frac{\left[kg(\epsilon)^2 - r_+^2 \left(\Lambda + \frac{\beta^2}{2} \right) \right] + \frac{4\beta q f(\epsilon) g(\epsilon) L_w^{3/2}}{15(1+L_w)} \left[(L_w + 5)\mathfrak{F}_{3+} - \frac{4}{3}L_w + \mathfrak{F}_{4+} + \frac{5}{4} \left(1 + \frac{3}{L_w^2} \right) \right]}{4\pi f(\epsilon) g(\epsilon) r_+}, & \text{ENED,} \\ \frac{\left[\beta^2 \ln\left(\frac{1+\Gamma_+}{2}\right) - \Lambda + \frac{kg(\epsilon)^2}{r_+^2} - \frac{(\Gamma_+^2 - 1)^2}{r_+} \left(\frac{8\mathfrak{F}_5}{45\Gamma_+} + \frac{2\beta^2}{9(\Gamma_+^2 - 1)} \left[\frac{(7+5\Gamma_+)}{(1-\Gamma_+)\Gamma_+} + 2\mathfrak{F}_{2+} \right] \right) + \frac{(\beta^2 r_+^4 (5\Gamma_+^2 - \frac{6}{\Gamma_+}) + 1)}{3(1-\Gamma_+)r_+^5} \right] r_+^2}{\pi f(\epsilon) g(\epsilon)}, & \text{LNED,} \\ \frac{\left[\frac{kg(\epsilon)^2}{r_+^2} - \Lambda - \frac{(2s-1)}{2} \left(\frac{\sqrt{2} q f(\epsilon) g(\epsilon) (2s-3)}{(2s-1)r_+^{2/(2s-1)}} \right)^{2s} \right] r_+}{4\pi f(\epsilon) g(\epsilon)}, & \text{PMI,} \end{cases} \quad (17)$$

with

$$\Upsilon = \begin{cases} \frac{2\beta^2 r^2}{3g(\epsilon)^2} [1 - \mathfrak{F}_{1+}], & \text{BINED,} \\ \frac{\beta^2 r^2}{6g(\epsilon)^2} \left[\frac{8\sqrt{\Gamma^2 - 1}}{5} \left(L_w^{\frac{3}{2}} \mathfrak{F}_3 + \frac{5(1+L_w)}{4\sqrt{L_w}} \right) - 1 \right], & \text{ENED,} \\ \frac{4\beta^2 r^2 (\Gamma - 1)}{3g(\epsilon)^2} \left[5 - \frac{\ln\left(\frac{\Gamma}{\Gamma+1}\right)}{(\Gamma-1)} + 4(\Gamma - 1)\mathfrak{F}_2 \right], & \text{LNED,} \\ -\frac{r^2 (2s-1)^2}{(4s-6)g(\epsilon)^2} \left(-\frac{\sqrt{2}(2s-3)qf(\epsilon)g(\epsilon)}{(2s-1)r^{2/(2s-1)}} \right)^{2s}, & \text{PMI,} \end{cases}$$

where $\mathfrak{F}_1 = {}_2F_1\left(\left[\frac{-1}{2}, \frac{-3}{4}\right], \left[\frac{1}{4}\right], 1 - \Gamma^2\right)$, $\mathfrak{F}_2 = {}_2F_1\left(\left[\frac{1}{2}, \frac{1}{4}\right], \left[\frac{5}{4}\right], 1 - \Gamma^2\right)$, and $\mathfrak{F}_3 = {}_2F_1\left(\left[1\right], \left[\frac{9}{4}\right], \frac{L_w}{4}\right)$ are the hyper-

geometric functions, and also m is an integration constant related to the total mass of the solutions.

3 Conserved and thermodynamic quantities

Considering the obtained solutions for different models of NED, this section is devoted to the calculation of the conserved and thermodynamical quantities and to the study of the effects of gravity's rainbow. Then we are going to expand our study to the stability of the solutions in a canonical ensemble.

Due to the fact that the employed metric only contains one temporal Killing vector, one can use the concept of surface gravity for calculating the temperature on the event horizon (r_+), which leads to

$$T = \frac{1}{2\pi} \sqrt{\nabla_\mu \chi_\nu \nabla^\mu \chi^\nu} = \frac{1}{4\pi} \frac{g(\epsilon)}{f(\epsilon)} \frac{d\Psi(r)}{dr} \Big|_{r=r_+}, \quad (16)$$

where the dependency on the rainbow functions indicates that the temperature is modified. Considering Eqs. (15) and (16), one can find

where $\Gamma_+ = \Gamma|_{r=r_+}$, $L_{w+} = L_w|_{r=r_+}$, $\mathfrak{F}_{1+} = \mathfrak{F}_1|_{r=r_+}$, $\mathfrak{F}_{2+} = \mathfrak{F}_2|_{r=r_+}$, $\mathfrak{F}_{3+} = \mathfrak{F}_3|_{r=r_+}$, $\mathfrak{F}_4 = {}_2F_1\left(\left[2\right], \left[\frac{13}{4}\right], \frac{L_{w+}}{4}\right)$, and $\mathfrak{F}_5 = {}_2F_1\left(\left[\frac{3}{2}, \frac{5}{4}\right], \left[\frac{9}{4}\right], 1 - \Gamma_+^2\right)$.

In order to study the entropy of the solutions, one can use the area law. It is easy to show that the entropy is

$$S = \frac{r_+^2}{4g(\epsilon)^2}. \quad (18)$$

On the other hand, even with the modifications in the metric, the entropy is independent of the electromagnetic fields. It is notable that although there is no trace of an electromagnetic field in explicit form of the entropy, the horizon radius is affected by the electromagnetic field under consideration.

As for the total charge of the solutions, one can employ the Gauss law. Considering this approach, one can show that,

for BI type models, the results are the same. In other words, in the case of BI type models, the total electric charge is independent of the nonlinearity parameter. For the PMI case, the total charge is modified and depends on the PMI parameter,

$$Q = \begin{cases} \frac{f(\epsilon)}{4\pi g(\epsilon)} q, & \text{BI type models,} \\ \frac{s(2s-1) \left(\frac{\sqrt{2}(2s-3)f(\epsilon)g(\epsilon)}{(2s-1)} \right)^{2s} q^{2s-1}}{8(3-2s)\pi f(\epsilon)g(\epsilon)^3}, & \text{PMI.} \end{cases} \tag{19}$$

In order to obtain the electric potential, we can calculate it on the horizon with respect to a reference

$$U = A_\mu \chi^\mu |_{r \rightarrow \infty} - A_\mu \chi^\mu |_{r \rightarrow r_+}, \tag{20}$$

which leads to

$$U = \begin{cases} \frac{q}{r_+} \mathfrak{F}_{2+}, & \text{BINED,} \\ \frac{4\beta\sqrt{L_{w+}} \left[\frac{45(3+L_{w+})}{8} + \frac{9L_{w+}(4+L_{w+})\mathfrak{F}_{3+}}{4} + L_{w+}^2 \mathfrak{F}_4 \right] r_+}{135g(\epsilon)f(\epsilon)(1+L_w)}, & \text{ENED,} \\ \frac{8\beta(\Gamma_+-1) \left[10\mathfrak{F}_{2+} + (\Gamma_+^2-1)\mathfrak{F}_5 \right] r_+ + \frac{2\beta[6(1-\Gamma_+)+(8-5\Gamma_+)]r_+}{9qf\Gamma_+}}{45q}, & \text{LNED,} \\ q r_+^{\frac{2s-3}{2s-1}}, & \text{PMI.} \end{cases} \tag{21}$$

It is worthwhile to mention that for $s \geq \frac{3}{2}$, the gauge potential is not well behaved, asymptotically. Therefore, we have both upper and lower limits for the nonlinearity parameter of PMI theory ($\frac{1}{2} < s < \frac{3}{2}$).

It is straightforward to show that the total finite mass of this black hole is

$$M = \frac{m}{8\pi f(\epsilon)g(\epsilon)}. \tag{22}$$

Here, we give more details for the examination of the first law of thermodynamics. Evaluating the metric function on the event horizon ($\psi(r = r_+) = 0$), one can obtain the geometrical mass (m) as a function of r_+ and q . Inserting $m(r_+, q)$ in Eq. (22), one finds

$$M = \begin{cases} \frac{\left[\frac{3k}{2} g(\epsilon)^2 + r_+^2 \left(\beta^2 \left[1 - \mathfrak{F}_{1\Delta} \right] - \frac{\Delta}{2} \right) \right] r_+}{12\pi f(\epsilon)g(\epsilon)^3}, & \text{BINED,} \\ \frac{\left[k g(\epsilon)^2 - r_+^2 \left(\Lambda + \frac{\beta^2}{2} \right) + \frac{\beta q f(\epsilon)g(\epsilon)}{3\sqrt{L_{w+}}} \left((1+L_{w+}) + \frac{4}{3} L_{w+}^2 \mathfrak{F}_{3+} \right) \right] r_+}{8\pi f(\epsilon)g(\epsilon)^3}, & \text{ENED,} \\ \frac{9kr_+^2 g(\epsilon)^2 + \beta^2 r_+^4 \left[4(\Gamma_+^2-1)\mathfrak{F}_{2+} - 5\Gamma_+ + 3\ln(1+\Gamma_+) \right] - 3 \left[\frac{\Delta}{4} + \beta^2 \left(\ln 2 - \frac{5}{3} \right) \right]}{18\pi r_+ f(\epsilon)g(\epsilon)^3}, & \text{LNED,} \\ \frac{\left[2 \left(k g(\epsilon)^2 - \frac{\Lambda r_+^2}{3} \right) - \frac{(2s-1)^2}{(2s-3)} \left(\frac{-\sqrt{2}(2s-3)\pi f(\epsilon)g(\epsilon)}{(2s-1)r_+^2} \right)^{2s} \right] r_+}{16\pi f(\epsilon)g(\epsilon)^3}, & \text{PMI.} \end{cases} \tag{23}$$

Now, we use Eqs. (18) and (19) to obtain $M = M(S, Q)$ in the following form:

$$M = \begin{cases} \frac{2 \left[\frac{3k}{8} + S \left(\beta^2 - \frac{\Delta}{2} \right) - S\beta^2 \mathfrak{F}_{1\Delta} \right] \sqrt{S}}{3\pi f(\epsilon)}, & \text{BINED,} \\ \frac{4 \left[\pi\beta Q \mathcal{L}_w^{3/2} \mathfrak{F}_{3\mathcal{L}} + \left(\frac{15k}{16} - \frac{5S}{8} (2\Lambda + \beta^2) \right) + \frac{5\pi\beta Q(1+\mathcal{L}_w)}{4\sqrt{\mathcal{L}_w}} \right] \sqrt{S}}{15\pi f(\epsilon)}, & \text{ENED,} \\ \frac{-16\pi^2 Q^2 \mathfrak{F}_{2\Delta} + \frac{3S(4S\Lambda-3k)}{4} + 12S^2\beta^2 \left[\ln \left(\frac{2}{1+\Delta} \right) + \frac{5(\Delta-1)}{3} \right]}{9\pi f(\epsilon)\sqrt{S}}, & \text{LNED,} \\ \frac{\left[\frac{3k}{4} - S\Lambda - \frac{3S(-2)^s (2s-1)^2}{2(2s-3)} \left(\frac{-\pi Q f(\epsilon)^s (3-2s)}{s^{2s-2} S} \right)^{2s/(2s-1)} \right] \sqrt{S}}{3\pi f(\epsilon)}, & \text{PMI,} \end{cases} \tag{24}$$

where $\mathfrak{F}_{1\Delta} = \mathfrak{F}_1 |_{\Gamma=\Delta}$, $\mathfrak{F}_{2\Delta} = \mathfrak{F}_2 |_{\Gamma=\Delta}$, and $\mathfrak{F}_{3\mathcal{L}} = \mathfrak{F}_3 |_{L_w=\mathcal{L}_w}$. Also, Δ and L_w are of the following forms:

$$\Delta = \sqrt{1 + \frac{\pi^2 Q^2}{\beta^2 S^2}},$$

$$\mathcal{L}_w = \text{LamberW} \left(\frac{4\pi^2 Q^2}{\beta^2 S^2} \right).$$

Now, we are in a position to study the validity of the first law of thermodynamics. Here, we should calculate $\left(\frac{\partial M}{\partial S} \right)_Q$ and $\left(\frac{\partial M}{\partial Q} \right)_S$, and then use Eqs. (18) and (19) to convert them as functions of r_+ and q . After some simplifications, one finds that these quantities are, respectively, the same as the temperature and potential which were obtained in Eqs. (17) and (21). Hence, although the rainbow functions affected thermodynamic and conserved quantities, the first law remains valid as

$$dM = \left(\frac{\partial M}{\partial S} \right)_Q dS + \left(\frac{\partial M}{\partial Q} \right)_S dQ. \tag{25}$$

4 Thermodynamic stability

In this section, we investigate the thermal stability conditions of nonlinearly charged black hole solutions in gravity’s rainbow. To do so, we investigate the heat capacity in terms of canonical ensemble. The thermal stability conditions are indicated by the sign of the heat capacity. The positivity of the heat capacity guarantees thermally stable solutions, whereas the negative heat capacity is considered to be an unstable state. Another advantage of studying the heat capacity is investigation of the phase-transition point. There is a limitation value for the minimum horizon radius (r_{+0}) and also a phase transition point; these are obtainable through calculating the root and divergence point of the heat capacity.

One can use the following relation for calculating the heat capacity:

$$C_Q = T \left(\frac{\partial S}{\partial T} \right)_Q = T \left(\frac{\frac{\partial S}{\partial r_+}}{\left(\frac{\partial T}{\partial r_+} \right)_Q} \right)_Q \tag{26}$$

Using the obtained values for the temperature and entropy for various models of NED (Eqs. (17) and (18)), one can find the following relations:

$$C_Q = \begin{cases} \frac{\left[\mathfrak{F}_{1++} + 2(\Gamma_+^2 - 1)\mathfrak{F}_{2+} - \frac{(kg(\epsilon)^2 + (2\beta^2 - \Lambda)r_+^2)}{2\beta^2 r_+^2} \right]}{4\pi\beta^2 g(\epsilon)^2 \left[\mathfrak{F}_{1++} + \frac{4(\Gamma_+^2 - 1)^2}{5}\mathfrak{F}_{5+} + \frac{(kg(\epsilon)^2 - (2\beta^2 - \Lambda)r_+^2)}{2\beta^2 r_+^2} \right]} r_+^2, & \text{BINED,} \\ \frac{r_+^2 (1 + L_{w+})^2 \mathcal{A}_1}{4\pi g^2(\epsilon) \mathcal{A}_2}, & \text{ENED,} \\ \frac{\beta^2 \Gamma_+^2 (1 - \Gamma_+) (\Gamma_+^2 - 1) \mathcal{B}_1 r_+^2}{128\pi g^2(\epsilon) (\mathcal{B}_2 + \mathcal{B}_3)}, & \text{LNED,} \\ \frac{\left(\left(s - \frac{1}{2} \right) \left[\frac{-\sqrt{2} q f(\epsilon) g(\epsilon) (2s-3)}{(2s-1)r_+^{2/(2s-1)}} \right] - \Lambda + \frac{kg(\epsilon)^2}{r_+^2} \right) r_+^2}{4\pi g(\epsilon)^2 \left(\left(s + \frac{1}{2} \right) \left[\frac{-\sqrt{2} q f(\epsilon) g(\epsilon) (2s-3)}{(2s-1)r_+^{2/(2s-1)}} \right] - \Lambda - \frac{kg(\epsilon)^2}{r_+^2} \right)}, & \text{PMI,} \end{cases} \tag{27}$$

where \mathcal{A}_1 , \mathcal{A}_2 , \mathcal{B}_1 , \mathcal{B}_2 , and \mathcal{B}_3 are

$$\mathcal{A}_1 = \beta q f(\epsilon) g(\epsilon) L_{w+}^2 \times \left[(5 - L_{w+}) \mathfrak{F}_{3+} + \frac{4L_{w+} \mathfrak{F}_{4+}}{9} - \frac{5(3 + L_{w+}^2)}{4L_{w+}^2} \right] - \frac{15L_{w+}^{1/2} (1 + L_{w+}) [kg^2(\epsilon) - r_+^2 (2\Lambda + \beta^2)]}{4},$$

$$\mathcal{A}_2 = -60\beta q f(\epsilon) g(\epsilon) L_{w+}^2 \times \left\{ (L_{w+}^3 + 3L_{w+}^2 - 9L_{w+} - 35) \mathfrak{F}_{5+} - \frac{16}{3} L_{w+} \left(L_{w+} + \frac{4}{3} \right) \mathfrak{F}_{4+} - \frac{32}{117} L_{w+}^2 (L_{w+} + 1) \mathfrak{F}_{6+} + \frac{5(L_{w+} - 1)}{4L_{w+}^2} (L_{w+}^3 + 5L_{w+}^2 + 15L_{w+} + 3) \right\} + \frac{15L_{w+}^{1/2} [kg^2(\epsilon) + r_+^2 (2\Lambda + \beta^2)]}{8} \times (L_{w+}^3 + 3L_{w+}^2 + 3L_{w+} + 1),$$

$$\mathcal{B}_1 = 9 \ln(2(1 + \Gamma_+)) + 4(1 - \Gamma_+^2) \times \left[\mathfrak{F}_{2+} + \frac{2}{5}(1 - \Gamma_+^2) \mathfrak{F}_{5+} \right] - \frac{9}{4\beta^2} \left(\Lambda - \frac{kg(\epsilon)^2}{r_+^2} \right) + \frac{3(6 - \Gamma_+ - 5\Gamma_+^3)}{(1 + \Gamma_+) \Gamma_+} + \frac{2(1 + \Gamma_+)(7 + 5\Gamma_+)}{\Gamma_+},$$

$$\mathcal{B}_2 = \frac{9\Gamma_+^3}{16\beta^6 r_+^4} \left[\frac{\beta^2(3 - \Gamma_+^2)}{2} - (\Gamma_+^2 - \Gamma_+ - 1) \right] - \frac{\ln(1 + \Gamma_+) \Gamma_+^2}{3r_+^{20}} - \frac{\beta^6 \Gamma_+^5 (\Gamma_+^2 - 1)^2}{2} \times \left\{ \frac{\left(\frac{(1+5\Gamma_+^2)}{4} \mathfrak{F}_{2+} - \frac{(\Gamma_+^2 - 1)(3+5\Gamma_+^2)}{5} \mathfrak{F}_{5+} \right)}{(\Gamma_+^2 - 1)} + \frac{(\Gamma_+^2 - 1)(1 + \Gamma_+^2) \mathfrak{F}_{7+}}{3\beta^2 g(\epsilon)^4} - \frac{9}{16\beta^4 \Gamma_+^2} \right. \\ \times \left[\frac{\left(\frac{17\beta^2}{3} - \frac{\Gamma_+^2}{r_+^4} - \frac{3(3-\Gamma_+^2)\ln 2}{4\beta^2 r_+^6} \right)}{(\Gamma_+^2 - 1)^2} + \frac{\left(\Lambda + \frac{kg(\epsilon)^2}{r_+^2} + \frac{32\beta^2(\Gamma_+^2 - 1)}{3} \right)}{2(\Gamma_+^2 - 1)^2} \right. \\ \left. \left. + \frac{3 \left(\frac{kg(\epsilon)^2}{r_+^2} - \frac{\Lambda}{3} \right) + \left(\Lambda + \frac{10kg(\epsilon)^2}{3r_+^2} + \frac{320\beta^2(\Gamma_+^2 - 1)}{9} \right)}{4(\Gamma_+^2 - 1)} \right] \right\},$$

$$\mathcal{B}_3 = \frac{\beta^4 \Gamma_+^2}{3} \left\{ \frac{-45\Gamma_+^5}{32} - \frac{3(\Gamma_+^2 - 1)\Gamma_+}{10} \right. \\ \times \left[-\frac{5(\Gamma_+^2 - 1)\Gamma_+^2}{2} \left(\mathfrak{F}_{2+} + \frac{2(1 - \Gamma_+^2) \mathfrak{F}_{5+}}{5} \right) + \frac{45}{32\beta^2} \left(4 \left[3 - \beta^2 \Gamma_+^2 \ln 2 + \frac{kg(\epsilon)^2}{4r_+^2} + \frac{23\beta^2(\Gamma_+^2 - 1)}{9} \right] \right. \right. \\ \left. \left. + \frac{(\Gamma_+^2 - 1)[kg(\epsilon)^2 - \Lambda r_+^2]}{r_+^2} \right) \right] + (\Gamma_+^2 - 1)\Gamma_+^4 \left(\frac{9\mathfrak{F}_{2+}}{4} - \frac{12(\Gamma_+^2 - 1)\mathfrak{F}_{5+}}{5} + (\Gamma_+^2 - 1)^2 \mathfrak{F}_{7+} \right) \\ - \frac{27(\Gamma_+^2 - 1)^2}{64\beta^2} \left[\frac{4(2 + \beta^4 \Gamma_+^4 \ln 2)}{\beta^2(\Gamma_+^2 - 1)^2} + \frac{\left(\Lambda + \frac{kg(\epsilon)^2}{r_+^2} + \frac{38\beta^2(\Gamma_+^2 - 1)}{3} \right)}{(\Gamma_+^2 - 1)^2} \right. \\ \left. \left. + \frac{2 \left(\Lambda + \frac{kg(\epsilon)^2}{r_+^2} + \frac{34\beta^2(\Gamma_+^2 - 1)}{9} \right)}{(\Gamma_+^2 - 1)} + \frac{\left(\Lambda + \frac{kg(\epsilon)^2}{r_+^2} + \frac{10\beta^2(\Gamma_+^2 - 1)}{9} \right)}{q^2} \right] \right\},$$

in which $\mathfrak{F}_7 = {}_2F_1 \left(\left[\frac{5}{2}, \frac{9}{4} \right], \left[\frac{13}{4} \right], 1 - \Gamma_+^2 \right)$.

In order to investigate the thermal stability of the solutions, we may regard explicit functional forms of the rainbow functions $f(\epsilon)$ and $g(\epsilon)$. The choices of these functions are motivated from various theoretical and phenomenological considerations. Here, we refer to more important forms which are based on interesting phenomenology.

The first model is related to constant speed of light and one may use it to solve the horizon problem [15, 16]. The functional form of both rainbow functions are the same

$$f(\epsilon) = g(\epsilon) = \frac{1}{1 - \lambda\epsilon}. \tag{28}$$

In addition, motivated by the results of loop quantum gravity and also non-commutative geometry, the rainbow functions are given by [107, 108]

$$f(\epsilon) = 1, \quad g(\epsilon) = \sqrt{1 - \eta\epsilon^n}. \tag{29}$$

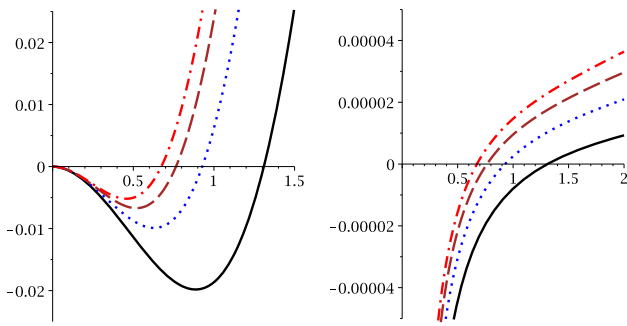


Fig. 1 ENED branch: C_Q (left panel) and T (right panel) versus r_+ for $k = 1, l = 1, \beta = 2, \varepsilon = 0.2$, and $q = 1$. $\xi = 0.5$ (continuous line), $\xi = 1$ (dotted line), $\xi = 1.5$ (dashed line), and $\xi = 2$ (dotted-dashed line)

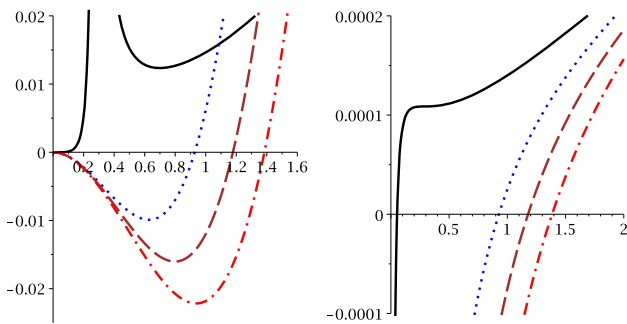


Fig. 2 ENED branch: C_Q (left panel) and T (right panel) versus r_+ for $k = 1, l = 1, \beta = 2, \varepsilon = 0.2$, and $\xi = 1$. $q = 0.1$ (continuous line), $q = 1$ (dotted line), $q = 1.5$ (dashed line), and $q = 2$ (dotted-dashed line)

Also, it was shown that in the non-commutative geometry context, it is better to regard a Gaussian trial functional form (exponential function) for $f(\varepsilon)$ to avoid a regularization/renormalization scheme [23,109]. On the other hand, based on the hard spectra from gamma-ray bursters, one may consider the rainbow functions [4] to have the following forms:

$$f(\varepsilon) = \frac{e^{\xi\varepsilon} - 1}{\xi\varepsilon}, \quad g(\varepsilon) = 1. \tag{30}$$

In order to study the thermodynamical behavior of the system, we use Eq. (30), in which $f(\varepsilon)$ has an exponential

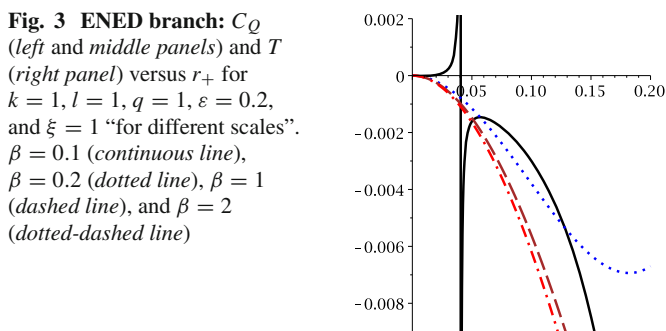


Fig. 3 ENED branch: C_Q (left and middle panels) and T (right panel) versus r_+ for $k = 1, l = 1, q = 1, \varepsilon = 0.2$, and $\xi = 1$ “for different scales”. $\beta = 0.1$ (continuous line), $\beta = 0.2$ (dotted line), $\beta = 2$ (dotted-dashed line)

form. Considering these two rainbow functions, we plot the following diagrams to study the effects of variation of different parameters on stability conditions and the phase transition of the obtained solutions (see Figs. 1, 2, 3, 4, 5).

In the case of BI type models, for specific values of different parameters, there is a region in which the temperature and heat capacity are negative. Black hole solutions are not physical in this region. In this case, the heat capacity enjoys a root, r_{+0} , in which for $r_+ > r_{+0}$, BI type black holes are in a stable state with positive temperature. r_{+0} is a decreasing function of ξ (Fig. 1) and an increasing function of the electric charge (Fig. 2). Interestingly, for small values of q , the heat capacity may enjoy a divergency which indicates a second order phase transition. Here, a phase transition of smaller to larger black holes takes place (continuous line in the left panel of Fig. 2). Surprisingly, the plotted diagram for the temperature in this case shows the existence of a subcritical isobar. The presence of subcritical isobars is observed for van der Waals-like liquid/gass systems. Such a behavior for black holes is only observed in the cases of considering cosmological constant as a thermodynamical pressure [106]. Here, without the use of an analogy between cosmological constant and thermodynamical pressure, we found the properties of the critical point.

In addition, we see that, for suitable choices of different parameters and small values of nonlinearity parameter, there are one root and two extrema in the temperature diagram; one minimum and one maximum. These extrema present themselves as divergencies in heat capacity diagrams. The stable states exist between the root and smaller divergency and after the larger divergency point (Fig. 3). Between the two divergencies, the heat capacity is negative while the temperature is positive, and therefore, in this region an unstable state exists. This instability switches to a stable state as the heat capacity meets the divergencies. In other words, a phase transition of smaller unstable to larger stable solutions takes place at the larger divergency point, while a phase transition of larger unstable to smaller stable solutions occurs at the smaller divergency point. Increasing the nonlinearity parameter leads to vanishing of these phase-transition points (Fig. 3).

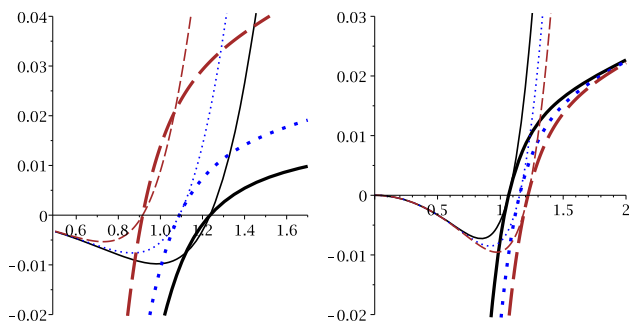


Fig. 4 PMI branch: C_Q and T (bold lines) versus r_+ for $k = 1, l = 1, \varepsilon = 0.2,$ and $s = 0.7$. Left panel: $q = 1, \xi = 0.5$ (continuous line), $\xi = 1$ (dotted line) and $\xi = 5$ (dashed line). Right panel $\xi = 1, q = 0.9$ (continuous line), $q = 1.3$ (dotted line), and $q = 1.7$ (dashed line)

It is worthwhile to mention that the small values of nonlinearity parameter represent a strong nonlinearity for the system. Therefore, as the nonlinearity of the system increases (the nonlinearity parameter decreases), the thermodynamical structure of the solutions will be modified. In addition, a numerical evaluation shows that the root of the heat capacity in LNEd theory is bigger comparing to other theories of the BI family. This indicates that physical stable solutions are obtained for higher values of the horizon radius for this theory of NED comparing to BINED and ENED. Oppositely, the divergence point in LNEd is located at a smaller horizon radius, which shows that black hole solutions in the presence of LNEd acquire thermal stability faster comparing to other two BI models.

For the PMI case, for specific values of the different parameters, like the BI case, a root is observed which is a limitation bound between non-physical and physical states. The value of the root is a decreasing function of ξ (Fig. 4, left panel) and an increasing function of the electric charge (Fig. 4, right panel). Interestingly, regarding the variation of s , for $0.5 < s < s_c$ ($s_c \approx 1.3$ for considered parameters), only a root (the mentioned bound point) exists (Fig. 5, left panel). As for $s = s_c$, there are two extrema, one minimum and one maximum, and also one root for the temperature (Fig. 5, middle and right panels). Between root and smaller divergence point and after the larger divergence point, the

heat capacity is positive and the system is in a stable state, whereas between two divergencies the system has a negative heat capacity (with positive T); hence, the black holes are not stable. Another interesting effect is that for $s_c < s < 1.5$, the smaller divergence point is a decreasing function of s , while the larger divergence is an increasing function of it (Fig. 5).

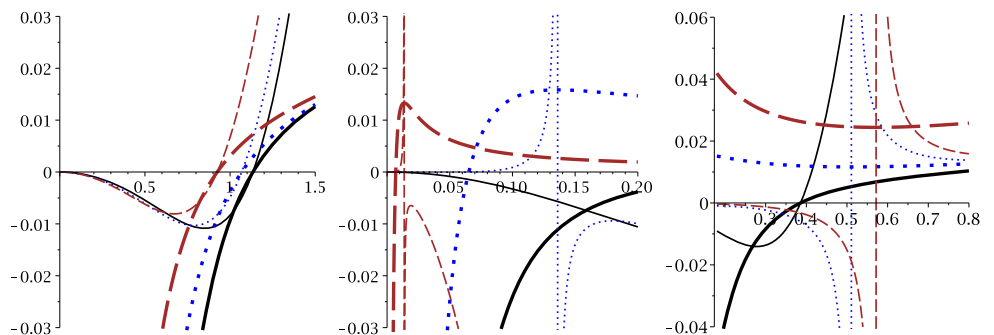
5 Closing remarks

In this paper, we have considered gravity’s rainbow in the presence of various models of NED. First, 4-dimensional black hole solutions for these configurations were derived, and then the related conserved and thermodynamic quantities were calculated. It was shown that some of the conserved and thermodynamical quantities were modified due to the contribution of gravity’s rainbow. Despite these modifications, the first law of thermodynamics was valid for these black hole solutions.

Next, we have studied the stability of the solutions and phase-transition points in the context of canonical ensemble. The employed nonlinear electromagnetic fields in this paper were categorized into two types: the BI type includes Born–Infeld, logarithmic and exponential forms, and the PMI model, is a power law generalization of the Maxwell Lagrangian.

In the case of BI types, we have found a lower bound for the horizon radius, r_{+0} , in which the black holes are not physical for $r_+ < r_{+0}$. Interestingly, for suitable choices of different parameters, we have found a second order phase-transition point which had characteristics of $T-V$ diagrams for a critical pressure (a subcritical isobar was observed). Then, by employing different parameters, we have found two extrema and a root in the temperature, and one root and two divergencies in the heat capacity diagrams. In this case, there exist two phase transitions of smaller unstable to larger stable and larger unstable to smaller stable solutions. The phase transitions took place at divergencies of the heat capacity. It was pointed out that the largest root and the smallest divergence point of the heat capacity belonged to the logarithmic form of NED.

Fig. 5 PMI branch: C_Q and T (bold lines) versus r_+ for $k = 1, l = 1, \varepsilon = 0.2, q = 1$ and $\xi = 1$ “for different scales”. Left panel $s = 0.9$ (continuous line), $s = 1$ (dotted line) and $s = 1.1$ (dashed line). Middle and right panels: $s = 1.3$ (continuous line), $s = 1.4$ (dotted line), and $s = 1.45$ (dashed line)



For the PMI case, similarly, stable physical and unstable non-physical states were observed for a range of s . Interestingly, for another range of this parameter the thermodynamical behavior was modified. A root, a maximum, and a minimum were observed for the temperature. In the places of these extrema (heat capacity enjoyed the existence of divergencies), two phase transitions of medium unstable to smaller or larger stable black holes took place. Another interesting property of this matter field was the effects of the variation of the s on divergencies of the heat capacity. For a specific range of s , the smaller divergence point was a decreasing function of s , while the larger divergency was an increasing function of the nonlinearity parameter.

It is evident that BI types and PMI models have different effects and contributions to the thermodynamical behavior of the black hole system. In other words, considering these two classes of NED leads to different modifications and properties for the system. In the case of BI family of NED, the theory under consideration will indicate the place of the formation of the stable solutions.

It will be worthwhile to study the solutions obtained in this paper in the context of extended phase space and investigate both modifications of gravity's rainbow and the nonlinear electromagnetic field for the critical behavior of the system. In addition, a generalization to higher dimensions is another interesting work. We left these issues for forthcoming work.

Acknowledgments We would like to thank the anonymous referee for useful suggestions and enlightening comments. We also thank the Shiraz University Research Council. This work has been supported financially by the Research Institute for Astronomy and Astrophysics of Maragha, Iran.

Open Access This article is distributed under the terms of the Creative Commons Attribution 4.0 International License (<http://creativecommons.org/licenses/by/4.0/>), which permits unrestricted use, distribution, and reproduction in any medium, provided you give appropriate credit to the original author(s) and the source, provide a link to the Creative Commons license, and indicate if changes were made. Funded by SCOAP³.

References

- V.A. Kosteletsky, S. Samuel, Phys. Rev. D **39**, 683 (1989)
- R. Gambini, J. Pullin, Phys. Rev. D **59**, 124021 (1999)
- S.M. Carroll, J.A. Harvey, V.A. Kosteletsky, C.D. Lane, T. Okamoto, Phys. Rev. Lett. **87**, 141601 (2001)
- G. Amelino-Camelia, J.R. Ellis, N.E. Mavromatos, D.V. Nanopoulos, S. Sarkar, Nature **393**, 763 (1998)
- G. 'tHooft, Class. Quantum Gravit. **13**, 1023 (1996)
- R. Iengo, J.G. Russo, M. Serone, JHEP **11**, 020 (2009)
- A. Adams, N. Arkani-Hamed, S. Dubovsky, A. Nicolis, R. Rattazzi, JHEP **10**, 014 (2006)
- B.M. Gripaos, JHEP **10**, 069 (2004)
- J. Alfaro, P. Gonzalez, R. Avila, Phys. Rev. D **91**, 105007 (2015)
- H. Belich, K. Bakke, Phys. Rev. D **90**, 025026 (2014)
- P. Horava, Phys. Rev. D **79**, 084008 (2009)
- P. Horava, Phys. Rev. Lett. **102**, 161301 (2009)
- M. Faizal, J. Phys. A **44**, 402001 (2011)
- M. Faizal, Mod. Phys. Lett. A **27**, 1250075 (2012)
- J. Magueijo, L. Smolin, Class. Quantum Gravit. **21**, 1725 (2004)
- J. Magueijo, L. Smolin, Phys. Rev. Lett. **88**, 190403 (2002)
- J.J. Peng, S.Q. Wu, Gen. Relativ. Gravit. **40**, 2619 (2008)
- W.G. Unruh, Phys. Rev. D **51**, 2827 (1995)
- R. Brout, S. Massar, R. Parentani, Ph. Spindel Phys. Rev. D **52**, 4559 (1995)
- S. Corley, T. Jacobson, Phys. Rev. D **54**, 1568 (1996)
- G. Amelino-Camelia, Int. J. Mod. Phys. D **11**, 1643 (2002)
- R. Garattini, Phys. Lett. B **685**, 329 (2010)
- R. Garattini, G. Mandanici, Phys. Rev. D **83**, 084021 (2011)
- A.F. Ali, Phys. Rev. D **89**, 104040 (2014)
- S.H. Hendi, M. Faizal, Phys. Rev. D **92**, 044027 (2015)
- S.H. Hendi. [arXiv:1507.04733](https://arxiv.org/abs/1507.04733)
- S.H. Hendi, M. Faizal, B. Eslam Panah, S. Panahiyan. [arXiv:1508.00234](https://arxiv.org/abs/1508.00234)
- A.F. Ali, M. Faizal, M.M. Khalil, JHEP **12**, 159 (2014)
- A.F. Ali, M. Faizal, M.M. Khalil, Nucl. Phys. B **894**, 341 (2015)
- S.H. Hendi, G.H. Bordbar, B. Eslam Panah, S. Panahiyan. [arXiv:1509.05145](https://arxiv.org/abs/1509.05145)
- R.J. Adler, P. Chen, D.I. Santiago, Gen. Relativ. Gravit. **33**, 2101 (2001)
- M. Cavaglia, S. Das, R. Maartens, Class. Quantum Gravit. **20**, L205 (2003)
- M. Cavaglia, S. Das, Class. Quantum Gravit. **21**, 4511 (2004)
- G. Amelino-Camelia, M. Arzano, A. Procaccini, Phys. Rev. D **70**, 107501 (2004)
- Y. Ling, X. Li, H.B. Zhang, Mod. Phys. Lett. A **22**, 2749 (2007)
- H. Li, Y. Ling, X. Han, Class. Quantum Gravit. **26**, 065004 (2009)
- V.A. De Lorenci, M.A. Souza, Phys. Lett. B **512**, 417 (2001)
- V.A. De Lorenci, R. Klippert, Phys. Rev. D **65**, 064027 (2002)
- M. Novello et al., Class. Quantum Gravit. **20**, 859 (2003)
- M. Novello, E. Bittencourt, Phys. Rev. D **86**, 124024 (2012)
- W. Heisenberg, H. Euler, Z. Phys. **98**, 714 (1936). (Translation by: W. Korolevski and H. Kleinert, Consequences of Dirac's Theory of the Positron). [arXiv:physics/0605038](https://arxiv.org/abs/physics/0605038)
- H. Yajima, T. Tamaki, Phys. Rev. D **63**, 064007 (2001)
- J. Schwinger, Phys. Rev. **82**, 664 (1951)
- D.H. Delphenich. [arXiv:hep-th/0309108](https://arxiv.org/abs/hep-th/0309108)
- D.H. Delphenich. [arXiv:hep-th/0610088](https://arxiv.org/abs/hep-th/0610088)
- E. Ayon-Beato, A. Garcia, Gen. Relativ. Gravit. **31**, 629 (1999)
- E. Ayon-Beato, A. Garcia, Phys. Lett. B **464**, 25 (1999)
- V.A. De Lorenci, R. Klippert, M. Novello, J.M. Salim, Phys. Rev. D **65**, 063501 (2002)
- I. Dymnikova, Class. Quantum Gravit. **21**, 4417 (2004)
- C. Corda, H.J. Mosquera, Cuesta. Mod. Phys. Lett. A **25**, 2423 (2010)
- C. Corda, H.J. Mosquera, Cuesta. Astropart. Phys. **34**, 587 (2011)
- H.H. Soleng, Phys. Rev. D **52**, 6178 (1995)
- H.P. Oliveira, Class. Quantum Gravit. **11**, 1469 (1994)
- D. Palatnik, Phys. Lett. B **432**, 287 (1998)
- E. Ayon-Beato, A. Garcia, Phys. Rev. Lett. **80**, 5056 (1998)
- H.J. Mosquera, J. Cuesta, M.Salim. Mon. Not. Roy. Astron. Soc. **354**, L55 (2004)
- H.J. Mosquera, J. Cuesta, M. Salim. Astrophys. J. **608**, 925 (2004)
- Z. Bialynicka-Birula, I. Bialynicka-Birula, Phys. Rev. D **2**, 2341 (1970)
- S.H. Hendi, B.E. Panah, S. Panahiyan. Phys. Rev. D **91**, 084031 (2015)
- S.H. Hendi, B.E. Panah, M. Momennia, S. Panahiyan. Eur. Phys. J. C **75**, 457 (2015)
- M. Born, L. Infeld, Proc. Roy. Soc. Lond. A **143**, 410 (1934)
- M. Born, L. Infeld, Proc. Roy. Soc. Lond. A **144**, 425 (1934)
- B. Hoffmann, Phys. Rev. **47**, 877 (1935)

64. M.H. Dehghani, N. Alinejadi, S.H. Hendi, Phys. Rev. D **77**, 104025 (2008)
65. M.H. Dehghani, S.H. Hendi, Phys. Rev. D **73**, 084021 (2006)
66. M. Allahverdizadeh, S.H. Hendi, J.P.S. Lemos, A. Sheykhi, Int. J. Mod. Phys. D **23**, 1450032 (2014)
67. R.G. Cai, Y.W. Sun, JHEP **09**, 115 (2008)
68. S.H. Mazharimousavi, M. Halilsoy, Z. Amirabi, Phys. Rev. D **78**, 064050 (2008)
69. R.G. Cai, D.W. Pang, A. Wang, Phys. Rev. D **70**, 124034 (2004)
70. S.H. Hendi, J. Math. Phys. **49**, 082501 (2008)
71. M.H. Dehghani, S.H. Hendi, A. Sheykhi, H. Rastegar Sedehi, JCAP **02**, 020 (2007)
72. M.H. Dehghani, S.H. Hendi, Int. J. Mod. Phys. D **16**, 1829 (2007)
73. M.H. Dehghani, H.R. Sedehi, Phys. Rev. D **74**, 124018 (2006)
74. S.H. Hendi, Phys. Rev. D **82**, 064040 (2010)
75. H.Q. Lu, L.M. Shen, P. Ji, G.F. Ji, N.J. Sun, Int. J. Theor. Phys. **42**, 837 (2003)
76. M.H. Dehghani, S.H. Hendi, Gen. Relativ. Gravit. **41**, 1853 (2009)
77. E.F. Eiroa, G.F. Aguirre, Eur. Phys. J. C **72**, 2240 (2012)
78. S.H. Hendi, Adv. High Energy Phys. **2014**, 697863 (2014)
79. J. Jing, S. Chen, Phys. Lett. B **686**, 68 (2010)
80. J. Jing, L. Wang, Q. Pan, S. Chen, Phys. Rev. D **83**, 066010 (2011)
81. S. Gangopadhyay, D. Roychowdhury, JHEP **05**, 156 (2012)
82. S. Gangopadhyay, D. Roychowdhury, JHEP **05**, 002 (2012)
83. S. Gangopadhyay, Mod. Phys. Lett. A **29**, 1450088 (2014)
84. W. Yao, J. Jing, JHEP **05**, 058 (2014)
85. E. Fradkin, A. Tseytlin, Phys. Lett. B **163**, 123 (1985)
86. R. Matsuvaev, M. Rahmanov, A. Tseytlin, Phys. Lett. B **193**, 205 (1987)
87. E. Bergshoeff, E. Sezgin, C. Pope, P. Townsend, Phys. Lett. B **188**, 70 (1987)
88. C. Callan, C. Lovelace, C. Nappi, S. Yost, Nucl. Phys. B **308**, 221 (1988)
89. O. Andreev, A. Tseytlin, Nucl. Phys. B **311**, 221 (1988)
90. R. Leigh, Mod. Phys. Lett. A **04**, 2767 (1989)
91. S.H. Hendi, JHEP **03**, 065 (2012)
92. S.H. Hendi, A. Sheykhi, Phys. Rev. D **88**, 044044 (2013)
93. S.H. Hendi, Adv. High Energy Phys. **2014**, 697914 (2014)
94. M. Hassaine, C. Martinez, Phys. Rev. D **75**, 027502 (2007)
95. M. Hassaine, C. Martinez, Class. Quantum Gravit. **25**, 195023 (2008)
96. H. Maeda, M. Hassaine, C. Martinez, Phys. Rev. D **79**, 044012 (2009)
97. S.H. Hendi, H.R. Rastegar-Sedehe, Gen. Relativ. Gravit. **41**, 1355 (2009)
98. S.H. Hendi, Phys. Lett. B **677**, 123 (2009)
99. S.H. Hendi, B.E. Panah, Phys. Lett. B **684**, 77 (2010)
100. S.H. Hendi, B.E. Panah, R. Saffari, Int. J. Mod. Phys. D **23**, 1450088 (2014)
101. S.W. Hawking, Phys. Rev. Lett. **26**, 1344 (1971)
102. J.M. Bardeen, B. Carter, S.W. Hawking, Commun. Math. Phys. **31**, 161 (1973)
103. J.D. Beckenstein, Phys. Rev. D **7**, 2333 (1973)
104. S.H. Hendi, S. Panahiyan, E. Mahmoudi, Eur. Phys. J. C **74**, 3079 (2014)
105. S.H. Hendi, S. Panahiyan, Phys. Rev. D **90**, 124008 (2014)
106. S.H. Hendi, S. Panahiyan, B.E. Panah, Int. J. Mod. Phys. Phys. D **25**, 1650010 (2016)
107. G. Amelino-Camelia, Liv. Rev. Relativ. **5**, 16 (2013)
108. U. Jacob, F. Mercati, G. Amelino-Camelia, T. Piran, Phys. Rev. D **82**, 084021 (2010)
109. R. Garattini, P. Nicolini, Phys. Rev. D **83**, 064021 (2011)